Organic Electronics 9 (2008) 968–973

Contents lists available at ScienceDirect

Organic Electronics

journal homepage: www.elsevier.com/locate/orgel

Polymer solar cells with poly(3,4-ethylenedioxythiophene) as transparent anode

Yi-Ming Chang [a], Leeyih Wang [a,b,*], Wei-Fang Su [a,b,c]

[a] Institute of Polymer Science and Engineering, National Taiwan University, Taipei 106, Taiwan
[b] Center for Condensed Matter Sciences, National Taiwan University, Taipei 106, Taiwan
[c] Department of Materials Sciences and Engineering, National Taiwan University, Taipei 106, Taiwan

ARTICLE INFO

Article history:
Received 3 June 2008
Received in revised form 3 July 2008
Accepted 5 July 2008
Available online 18 July 2008

PACS:
73.61.Ph
78.66.Qn
84.60.Jt

Keywords:
Polymer solar cells
Polymer electrode
Conjugated polymers
Poly(3,4-ethylenedioxythiophene)

ABSTRACT

A highly conductive poly(3,4-ethylenedioxythiophene) (PEDOT) film was prepared by *in-situ* oxidative polymerization on a glass substrate and adopted as the transparent anode of polymer solar cells that were based on a blend of poly(3-hexylthiophene) (P3HT) and [6,6]-phenyl C_{61} butyric acid methyl ester (PCBM) as the photoactive layer. PEDOT anodes of various thicknesses were prepared for use in such devices. The resistance of the PEDOT and the transmitted light intensity of the irradiation varied with the thickness. The best devices exhibited a power conversion efficiency of 2.6% under simulated AM1.5G solar irradiation. Importantly, the conversion efficiency of incident photons to electrons in the device with the PEDOT anode was comparable to that with an ITO electrode, indicating the practicability of applying PEDOT as anode to fabricate high-efficiency flexible solar cells.

1. Introduction

In recent years, considerable research has focused on developing polymer solar cells [1–5] because they can be potentially laminated onto mobile phones, personal digital assistants (PDA) and laptops, to provide trickle electricity, reducing the need to plug them in for power. Eventually, such flexible polymer solar cells will be able to integrate into clothes, powering electric appliances on a person. However, indium tin oxide (ITO) is still widely used as transparent electrodes of polymer-based solar cells and other optoelectronic devices because of its low resistance and high optical transparency. Although an ITO electrode provides many advantages in the fabrication of polymer solar cells, its brittleness and thermal expansion coefficient limit its flexibility and thermal stability on a polymer substrate, and are responsible for poor interfacial compatibility between the organic materials and ITO surface [6,7]. Moreover, the high material and production costs of ITO engender a strong desire to develop a solution processable and low-cost material as the transparent electrode of polymer solar cells.

Recently, transparent films of carbon nanotubes (CNTs) have been used as electrodes in organic optoelectronic devices. Rowell et al. demonstrated a poly(3-hexylthiophene) (P3HT)/[6,6]-phenyl C_{61} butyric acid methyl ester (PCBM) solar cell using a transparent metallic single-wall CNT on plastic substrate as anode [8]. Such devices showed the highest power conversion efficiency of 2.5%. This performance is comparable to the reference device with ITO anode. Nevertheless, although transparent CNTs electrodes have high optical transparency and high conductivity, the

* Corresponding author. Address: Institute of Polymer Science and Engineering, National Taiwan University, No. 1, Sec. 4, Roosevelt Road, Taipei 106, Taiwan. Tel.: +886 2 33665291; fax: +886 2 23696221.
E-mail address: leewang@ntu.edu.tw (L. Wang).

1566-1199/$ - see front matter © 2008 Elsevier B.V. All rights reserved.
doi:10.1016/j.orgel.2008.07.003

high cost and difficulty of its process limit their practical use in commercial products. Very recently, a polymer solar cell with graphene-based film as anode was also reported but its efficiency is still much less than 1% [9]. Accordingly, one of the important advantages of using semiconductive conjugated polymer as a transparent electrode is that conducting polymers can be easily fabricated by inkjet printing, screen printing, roll-to-roll coating or other economical solution processes [10–12].

Among the numerous conducting polymers, the polythiophene derivative, poly(3,4-ethylenedioxythiophene) (PEDOT) has high conductivity and excellent environmental stability, but it is insoluble in many solvents. Water-dispersible PEDOT:poly(styrenesulfonate) (PSS) complex has been extensively used as a hole-transport layer in organic optoelectronic devices because of its ease of process and suitable work function [13]. PEDOT:PSS exhibits significant optical transparency to visible light of 80% [14], and its conductivity can be improved by the addition of polyalcohols or high dielectric solvents [15–21]. Several polymer solar cells using PEDOT:PSS as a transparent electrode have recently been demonstrated [16,20–22]. However, its highest conductivity is still about 20 times of magnitude lower than that of ITO (~3800 S/cm) [20].

Although PEDOT:PSS has shown favorable optical transparency, its conductivity is still too low to support high device performance because of the existence of insulating PSS component. Winther-Jensen and West recently synthesized a PEDOT thin film without insulating PSS by vapor-phase polymerization [23]. This process utilizes iron(III) toluenesulfonate ($Fe(OTs)_3$) as an oxidant and pyridine as a basic inhibitor. The polymer solar cells based on such PEDOT electrodes exhibit usable device performance [24]. In addition, Ha et al. demonstrated a simple process for preparing highly conductive PEDOT thin films on a glass substrate [25]. This method utilizes iron(III) toluenesulfonate ($Fe(OTs)_3$) as an oxidant and imidazole as a base to reduce the reactivity of $Fe(OTs)_3$, reducing the rate of polymerization and the doping level. At optimal conduction, the conductivity of this PEDOT thin film is approximately 750 S/cm. This easily prepared and highly conductive PEDOT electrode can be further applied in the soft electronics industry, in which inorganic materials are unsuitable. This work demonstrates a series of P3HT:PCBM-based solar cells with PEDOT anode of various thicknesses (Fig. 1) and measures their current–voltage characteristics, including their solar power conversion efficiency, resistance and incident photon to electron conversion efficiency (IPCE), to investigate the effect of light intensity, PEDOT transparency and sheet resistance.

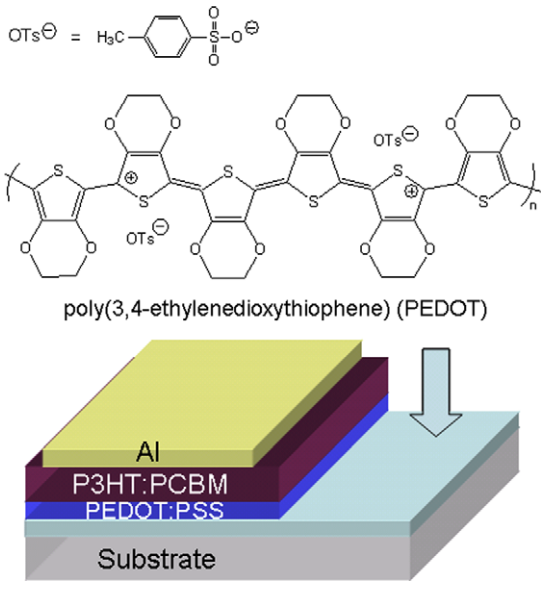

Fig. 1. Schematic representation of the P3HT:PCBM-based solar cell with PEDOT anode.

2. Experimental

The PEDOT films were polymerized in a manner similar to that employed by Ha et al. [25]. 3,4-Ethylenedioxythiophene (EDOT) (Baytron M, Bayer) was first purified by distillation, yielding a clear colorless liquid, and the glass substrate was cleaned with detergent, acetone and isopropyl alcohol in an ultrasonic bath, before being dried in an oven. $Fe(OTs)_3$ (4 g, 40 wt.% in *n*-butanol, Baytron C, Bayer) and imidazole (0.36 g, 5.25 mmol) were dissolved in *n*-butanol (7.4 mL) with stirring at 50 °C for 30 min. The distilled EDOT (0.43 g, 3.00 mmol) was then added to the solution. The mixture was rapidly spin-coated onto the pre-cleaned glass substrate at various spin rates, and then moved onto a digitally controlled hotplate for EDOT polymerization at 110 °C for 1 h. Finally, the PEDOT/glass substrates were cooled to room temperature. They were washed twice with methanol to remove the residual imidazole and oxidant and then dried on a hot plate at 110 °C for 5 min. Regioregular P3HT was prepared using the Grignard metathesis approach, providing regiocontrol in each coupling step in the polymeric reaction [26]. The regioregularity was determined by ^{1}H NMR to be greater than 96%. The number-average molecular weight was 43000 g/mol and the polydispersity index was 1.5, based on GPC analysis (THF eluent, polystyrene standard). PCBM was prepared in our laboratory using a method described elsewhere [27].

Polymer solar cells with an ITO (15 Ω/sq, Merck Display) or PEDOT anode were prepared as follows. PEDOT transparent films of various thicknesses were prepared as in the above experiment without further cleaning. The ITO glass was cleaned as the glass substrate described above. PEDOT:PSS (Baytron P, Bayer) was spin-coated on thus-prepared anode substrates to modify the anode surface, affording a hole-collection layer of 60 nm, after drying at 140 °C for 10 min. Then, the P3HT:PCBM blend (10 mg P3HT and 8 mg PCBM in 1 mL chlorobenzene) was spin-coated on top of the hole-collection layer at 700 rpm for 60 s, forming an active layer with a thickness of 90 nm. A 100 nm aluminum electrode was then deposited on top of the active layer using a thermal evaporator. The active area of the device, defined using a shadow mask was 0.09 cm^2. After the cathode was deposited, the devices were annealed using a digitally controlled hotplate at 150 °C for 30 min, and then slowly cooled to room temperature.

The optical transparent spectra of the PEDOT films on glass substrate were measured using a Hitachi U-3410 spectrophotometer. The surface morphology of the electrode films was observed by atomic force microscopy (AFM) using a Digital Instruments NanoScope IIIa. All images were captured in height-contrast mode, revealing the surface roughness of the films. The sheet resistances of PEDOT films were measured using a four-point probe meter, Quatek QT50, and the thickness of each sample was measured using a Dektak 6 M profilometer after a cut had been made on the film surface by a razor blade to expose the glass surface. Averages of at least four measurements made at different locations on the sample were taken to determine film thickness and calculate sheet resistance. The work functions of materials were measured using an AC2 photoelectron spectrometer (Riken Keiki Co.). The ITO sample was cleaned before any measurement was made. The PEDOT sample was prepared as in the above experiment and without further cleaning.

The current–voltage characteristics were measured using a Keithley 236 source measurement unit. The solar simulator comprised an Oriel xenon arc lamp with an AM1.5G solar filter, and the intensity was calibrated using a mono-Si reference cell with a KG5 color filter. A set of neutral density filters with a constant optical density over the spectral range of the light source was used to vary the light intensity from 50 mW/cm^2 to 6 mW/cm^2. The IPCE spectra were recorded under illumination by a xenon lamp with a monochromator (TRIAX 180, JOBIN YVON), and the light intensity was calibrated using an OPHIR 2A-SH power meter.

3. Results and discussion

In-situ oxidative polymerization was adopted to prepare PEDOT films on glass substrate using $Fe(OTs)_3$ and imidazole as oxidant and base, respectively. The function of imidazole is to reduce the reduction potential of the Fe^{3+}/Fe^{2+} couple and then the polymerization rate by reducing the pH of a reaction medium and forming a coordination complex with $Fe(OTs)_3$. Additionally, the presence of imidazole promotes formation of polymer chains with high molecular weights through a faster quench on monomer radicals than on oligomeric radicals during polymerization, thus increasing the conductivity of the PEDOT film [25]. The as-synthesized polymer film did not dissolve in water and common organic solvents, preventing the dissolution of PEDOT in the subsequent device fabrication process. The surface roughness of the PEDOT film was determined from its AFM images, shown in Fig. 2. It was found to be around 1.5 nm which was ~3.1 nm less than that of the ITO surface (The AFM image of the ITO surface is not shown.).

PEDOT films of four thicknesses were obtained by varying the spin rates – 256 nm, 169 nm, 81 nm and 28 nm. Fig. 3 plots the sheet resistances and transparency of the PEDOT films on a glass substrate. The sheet resistances were measured by the four-point probe method. The results show that the sheet resistances increased as the PEDOT film thickness decreased. The values ranged from 76 to

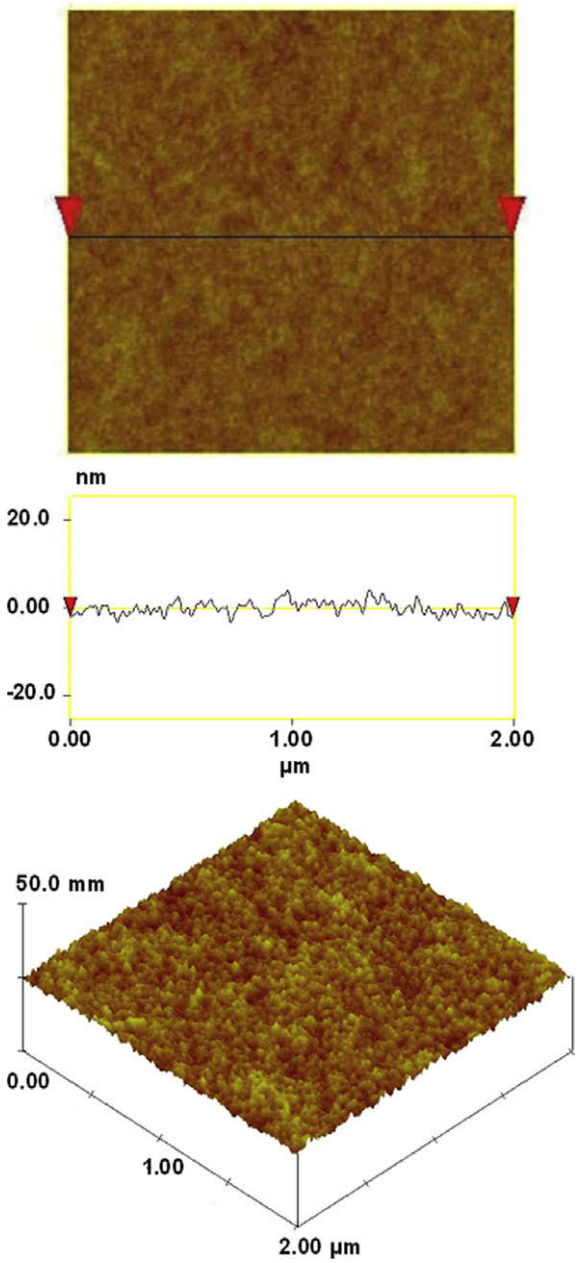

Fig. 2. AFM images of the PEDOT film.

761 Ω/sq, and corresponding to thicknesses of 256–28 nm, with an average conductivity of about 500 S/cm. In these cases, the conductivity of PEDOT was closer to, but lower than, that of ITO (15 Ω/sq, 3800 S/cm), but it still exceeded those of the other doped PEDOT:PSS conductive materials, presented in the literature [15–21]. The absorption spectrum of photoactive P3HT has a main absorption wavelength in the range of 400–650 nm with a maximum absorption wavelength at 510 nm. Therefore, Fig. 3 also plots the transmittance of PEDOT film on glass at the wavelength of 510 nm to examine the effect of PEDOT on the absorbance of P3HT in a polymer solar cell. As expected,

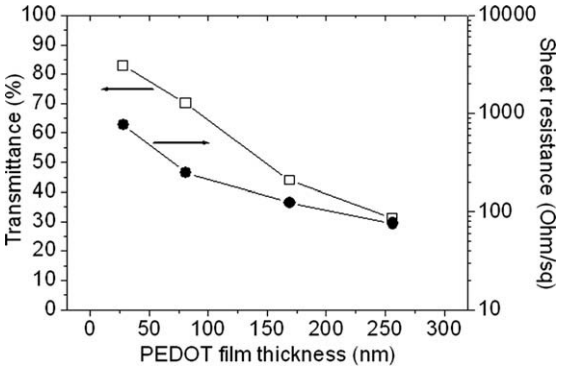

Fig. 3. The influences of the thickness of PEDOT film on its transmittance at 510 nm (□) and sheet resistance (●).

the transmittance increased as PEDOT film thickness declined, allowing more sunlight to penetrate to the active layer of the solar cells. Thinner PEDOT electrodes can act positively as transparent electrodes with good transmittance; however, the larger resistance increases the total series resistance of the diodes. Obviously, the primary task in improving device efficiency is to identify the optimal balance condition between thickness and resistance.

The work function of the electrode material is also a key parameter in determining device performance. In this work, a UV source was employed to measure the ionization potential of materials in air using an AC2 photoelectron spectrometer. Fig. 4 plots the square root of the counting rate (CR) as a function of the photon energy and the photoemission threshold energy, which is also called the work function, was determined from the crossing point of the background and the yield line. The work functions of PEDOT and ITO were found out to be 4.97 eV and 4.94 eV, respectively. Because measurements of the samples were made in air, the value of ITO measured herein was slightly higher than that reported in the literature, ~4.7 eV, as determined by ultraviolet photoelectron spectroscopy in an ultra-high vacuum [7,28]. Since the work function of the as-prepared PEDOT is very close to that of ITO, the additional adjustment on energy levels of photoactive ingredients can be minimized as using PEDOT replaces ITO as the anode of photovoltaic cells. Herein, a series of devices with a PEDOT/PEDOT:PSS/P3HT:PCBM/Al structure (as shown in Fig. 1) were fabricated to investigate the effect of the thickness of the PEDOT anode on device performance.

An ideal high-efficiency solar cell would have a series resistance (R_S) of close to zero [29]. For a real solar cell, a smaller R_S is associated with a better fill factor (FF) and short circuit current density (J_{SC}), and therefore higher power conversion efficiency (PCE) of devices [29,30]. The calculation of R_S from the dark current–voltage curves of the devices with various PEDOT thicknesses (Fig. 5) reveals that the R_S of the PEDOT anode-based devices increased as the PEDOT thickness declined. The values ranged from 40 to $10^3\ \Omega\ cm^2$ and corresponded to electrode thicknesses of 256–28 nm; they remained higher than that of the ITO anode-based device (<10 $\Omega\ cm^2$). R_S varies in a manner similar to the sheet resistance of PEDOT films (Fig. 3) because R_S is the sum of the contact resistance and the bulk resistance of the materials, ($R_S = R_{anode} + R_{PEDOT:PSS} + R_{P3HT} + R_{PCBM} + R_{Al}$) [31]. All devices were fabricated with the same photoactive components under identical process, so it is reasonable to assume that the resistances of PEDOT:PSS, P3HT:PCBM and Al stayed constant in devices. Therefore, the R_S of the device changes only with the sheet resistance of the PEDOT anode.

Fig. 6a–d display the effect of PEDOT film thickness on the open-circuit voltage (V_{OC}), FF, J_{SC} and PCE of the devices under AM 1.5G illumination at various light intensities. Fig. 6a demonstrates that the anode thickness does not affect V_{OC} when the light intensity is fixed. However, when the light intensity increases from 6, 18, 29, 38 to 50 mW/cm^2; V_{OC} monotonically increases from 0.41, 0.47, 0.50, 0.52 to 0.54 V, respectively, as for general polymer solar cells [32,33]. Fig. 6b plots the dependence of FF on the PEDOT thickness under various light intensities. For fixed anode thickness, the FF of the PEDOT anode-based devices increased slightly as the light intensity decreased, which characteristic is similar to that of typical solar cells [33]. The data also indicate that the FF fell from ~36% to ~25% as the PEDOT thickness decreased from 256 to 28 nm, because a thinner anode thickness leads to a higher sheet resistance and a higher R_S. Fig. 6c plots the dependence of J_{SC} on the PEDOT anode thickness under different light intensities. As expected, J_{SC} increased as the light intensity

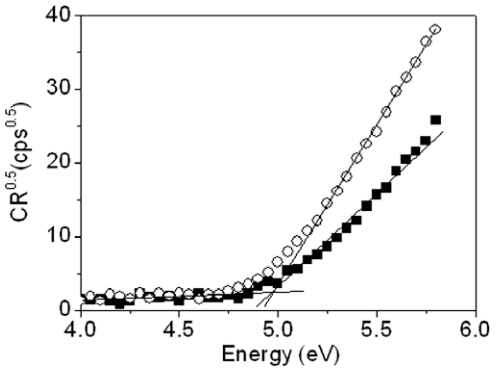

Fig. 4. Photoelectron yield spectroscopy for PEDOT (○) and ITO (■) films.

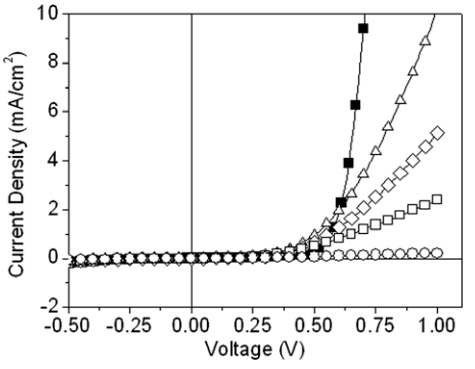

Fig. 5. Dark current characteristics of anode/PEDOT:PSS/P3HT:PCBM/Al devices with different anodes: ITO (■); PEDOT with thicknesses of 256 nm (△); 169 nm (◇); 81 nm (□); and 28 nm (○).

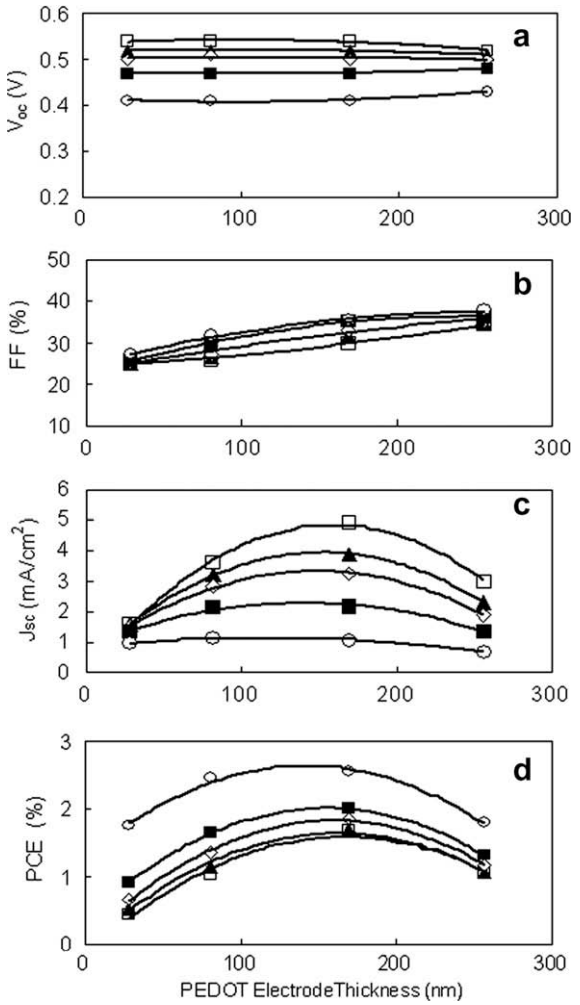

Fig. 6. Dependence of (a) open-circuit voltage (V_{OC}), (b) fill factor (FF), (c) short-circuit current density (J_{SC}) and (d) power conversion efficiency (PCE) on the thickness of PEDOT anode in the anode/PEDOT:PSS/P3HT:PCBM/Al devices under AM1.5G solar simulated irradiation at power intensities of 50 mW/cm^2 (□); 38 mW/cm^2 (▲); 29 mW/cm^2 (◇); 18 mW/cm^2 (■); and 6 mW/cm^2 (○).

raised from 6 to 50 mW/cm^2 (Fig. 6c). J_{SC} also increased with PEDOT anode thickness from 28 to 169 nm because a thicker PEDOT has a lower resistance and yields a higher J_{SC}. However, as the PEDOT anode thickness continues to increase to 256 nm, the resistance may become favorable, but a thicker film corresponds to an inferior transmittance, and therefore poor light absorption and photocurrent generation, causing the photocurrent of a 256 nm-thick PEDOT anode-based device to be lower than that of a 169 nm-thick device. Accordingly, J_{SC} is largest for a PEDOT anode-based device with a thickness of 169 nm, suggesting that the PEDOT anode has the optimal balance between the transmittance and the resistance at this thickness. In brief, as the cell is operated under a high-intensity illumination, a thicker PEDOT associated with a lower sheet resistance will conduct more photocurrent out of the cell. Conversely, as the cell is illuminated with a low-intensity

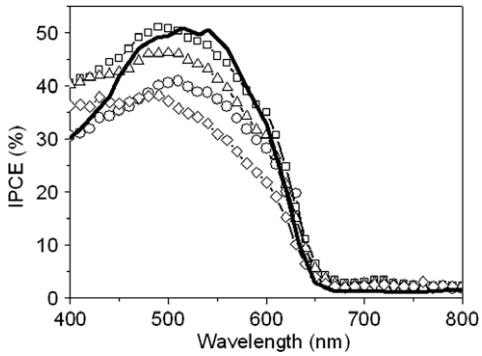

Fig. 7. (a) Incident photon-to-current conversion efficiency (IPCE) spectra of anode/PEDOT:PSS/P3HT:PCBM/Al devices with different anodes: ITO (black line), 256 nm-thick PEDOT (◇), 169 nm-thick PEDOT (△), 81 nm-thick PEDOT (□) and 28 nm-thick PEDOT (○).

light, a thinner PEDOT will allow more light to reach the photoactive layer and produce more excitons and, thus, increase photocurrent. Therefore, at a fixed light intensity, PEDOT thickness must be carefully adjusted to balance the series resistance of the cell and the exciton generation rate inside the photoactive layer to optimize cell efficiency. Fig. 6d plots the calculated PCE of devices with various PEDOT thicknesses under different light intensities. Basically, the trend is similar to those of V_{OC}, FF and J_{SC}. Since the resistance limited the photocurrent output under high light intensity, PEDOT anode-based devices herein perform best when the anode thickness is 169 nm under 6 mW/cm^2 of AM 1.5G irradiation; the highest PCE is 2.6% with an FF of 35.5%.

Fig. 7 presents the IPCE spectra of the devices with an anode/PEDOT:PSS/P3HT:PCBM/Al structure using ITO or PEDOT of various thicknesses as the anode. The efficiency under monochromatic illumination with a power density of 63–480 μW/cm^2, depending on the irradiation wavelength, was calculated. All IPCE curves closely follow the absorption spectrum of the P3HT:PCBM blend and maximum efficiency wavelength of the IPCE located at around 500 nm. The IPCE spectra of the devices were sensitive to the change in PEDOT anode thickness. When the PEDOT anode thickness was 81 nm, the IPCE reached maxima over the full range of wavelengths due to the optimal equilibrium between the sheet resistance and the light transmittance. Very interestingly, these IPCEs were comparable to those of the ITO anode-based device, directly establishing the feasibility of using this organic-based PEDOT as the anode in fabricating high-efficiency flexible devices.

4. Conclusions

This work demonstrated a polymer solar cell with a conductive PEDOT anode synthesized by *in-situ* polymerization of EDOT on a glass substrate using $Fe(OTs)_3$ and imidazole as oxidant and base, respectively. The results reveal that the thickness of PEDOT is a key factor in determining the device performance. Thinner PEDOT electrodes are more effective transparent electrodes with better transmittance,

allowing more sunlight to be incident on the active layer of the solar cells, but increasing the series resistance, thus reducing the photocurrent of the devices. Thicker PEDOT electrodes have a lower resistance, but transmittance limits the sunlight absorption of the devices. When the thickness of the PEDOT anode is optimized, a PCE of 2.6%, under AM1.5G irradiation is obtained. Furthermore, the IPCE results demonstrate that these PEDOT anode-based devices have a similar efficiency to that of an ITO anode-based device, suggesting the feasibility of replacing ITO with PEDOT as the anode of a polymer solar cell. This transparent and flexible polymer electrode can be further used to develop completely organic solar cells or other electronic devices using an easy and economic solution process on flexible plastic substrates.

Acknowledgements

The authors would like to thank National Taiwan University, Academia Sinica and National Science Council of Republic of China for financially supporting this research.

References

[1] C.J. Brabec, N.S. Sariciftci, J.C. Hummelen, Adv. Funct. Mater. 11 (2005) 15.
[2] H. Spanggaard, F.C. Krebs, Sol. Energy Mater. Sol. Cells 83 (2004) 125.
[3] E. Bundgaard, F.C. Krebs, Sol. Energy Mater. Sol. Cells 91 (2007) 954.
[4] S. Günes, H. Neugebauer, N.S. Sariciftci, Chem. Rev. 107 (2007) 1324.
[5] B.C. Thompson, J.M.J. Fréchet, Angew. Chem. Int. Ed. 46 (2007) 2.
[6] J.S. Kim, M. Granström, R.H. Friend, N. Johansson, W.R. Salaneck, R. Daik, W.J. Feast, J. Appl. Phys. 84 (1998) 6859.
[7] M.G. Mason, L.S. Hung, C.W. Tang, S.T. Lee, K.W. Wong, M. Wang, J. Appl. Phys. 86 (1999) 1688.
[8] M.W. Rowell, M.A. Topinka, M.D. McGehee, H. Prall, G. Dennler, N.S. Sariciftci, L. Hu, G. Gruner, Appl. Phys. Lett. 86 (2006) 233506.
[9] X. Wang, L. Zhi, N. Tsao, Z. Tomović, J. Li, K. Müllen, Angew. Chem. Int. Ed. 47 (2008) 2990.
[10] C.N. Hoth, S.A. Choulis, P. Schilinsky, C.J. Brabec, Adv. Mater. 19 (2007) 3973.
[11] F.C. Krebs, J. Alstrup, H. Spanggaard, K. Larsen, E. Kold, Sol. Energy Mater. Sol. Cells 83 (2004) 293.
[12] S.S. Kim, S.I. Na, J. Jo, G. Tae, D.Y. Kim, Adv. Mater. 19 (2007) 4410.
[13] J.S. Huang, P.F. Miller, J.S. Wilson, A.J. de Mello, J.C. de Mello, D.D.C. Bradley, Adv. Funct. Mater. 15 (2005) 290.
[14] B.L. Groenendaal, F. Jonas, D. Freitag, H. Pielartzik, J.R. Reynolds, Adv. Mater. 12 (2000) 481.
[15] L.A.A. Pettersson, S. Ghosh, O. Inganäs, Org. Electron. 3 (2002) 143.
[16] F. Zhang, M. Johansson, M.R. Andersson, J.C. Hummelen, O. Inganäs, Adv. Mater. 14 (2002) 662.
[17] W.H. Kim, A.J. Makinen, N. Nikolov, R. Shashidhar, H. Kim, Z.H. Kafafi, Appl. Phys. Lett. 80 (2002) 3844.
[18] J.Y. Kim, J.H. Jung, D.E. Lee, J. Joo, Synth. Met. 126 (2002) 311.
[19] S.K.M. Jönsson, J. Birgerson, X. Grispin, G. Greczynski, W. Osikowicz, A.W.D. van der Gon, W.R. Salaneck, M. Fahlman, Synth. Met. 139 (2003) 1.
[20] J. Quyang, C.W. Chu, F.C. Chen, Q. Xu, Y. Yang, Adv. Funct. Mater. 15 (2005) 203.
[21] E. Ahlswede, W. Mühleisen, M.W. bin Moh Wahi, J. Hanisch, M. Powalla, Appl. Phys. Lett. 92 (2008) 143307.
[22] B. Zimmermann, M. Glatthaar, M. Niggemann, M.K. Riede, A. Hinsch, A. Gombert, Sol. Energy Mater. Sol. Cells 91 (2007) 374.
[23] B. Winther-Jensen, K. West, Macromolecules 37 (2004) 4538.
[24] B. Winther-Jensen, F.C. Krebs, Sol. Energy Mater. Sol. Cells 90 (2006) 123.
[25] Y.H. Ha, N. Nikolov, S.K. Pollack, J. Mastrangelo, B.D. Martin, R. Shashidhar, Adv. Funct. Mater. 14 (2004) 615.
[26] R.S. Loewe, S.M. Khersonsky, R.D. McCullough, Adv. Mater. 11 (1999) 250.
[27] J.C. Hummelen, B.W. Knight, F. Lepeq, F. Wudl, J. Org. Chem. 60 (1995) 532.
[28] D.J. Milliron, I.G. Hill, C. Shen, A. Kahna, J. Schwartz, J. Appl. Phys. 87 (2000) 572.
[29] C.J. Brabec, V. Dyakonov, J. Parisi, N.S. Sariciftci, Organic Photovoltaics: Concepts and Realization, Springer, New York, 2003. Chapter 5, pp. 214.
[30] W. Ma, C.Y. Yang, X. Gong, K. Lee, A.J. Heeger, Adv. Funct. Mater. 15 (2005) 1617.
[31] J. Rostalski, D. Meissner, Sol. Energy Mater. Sol. Cells 63 (2000) 37.
[32] L.J.A. Koster, V.D. Mihailetchi, R. Ramaker, P.W.M. Blom, Appl. Phys. Lett. 86 (2005) 123509.
[33] J.Y. Kim, K. Lee, N.E. Coates, D. Moses, T.Q. Nguyen, M. Dante, A.J. Heeger, Science 317 (2007) 222.